Malaysian Journal of Analytical Sciences, Vol 23 No 1 (2019): 100 - 108
DOI: https://doi.org/10.17576/mjas-2019-2301-12

MALAYSIAN JOURNAL OF ANALYTICAL SCIENCES
Published by The Malaysian Analytical Sciences Society
ISSN 1394 - 2506

SYNTHESIS AND CHARACTERIZATION OF $SrSnO_3$ USING DIFFERENT SYNTHESIS METHODS

(Sintesis dan Pencirian $SrSnO_3$ yang Dihasilkan Melalui Kaedah Sintesis Berlainan)

Muhammad Arif Riza, Suhaila Sepeai, Norasikin Ahmad Ludin, Mohd Asri Mat Teridi, Mohd Adib Ibrahim*

Solar Energy Research Institute (SERI)
Universiti Kebangsaan Malaysia, 43600 UKM Bangi, Selangor, Malaysia

**Corresponding author: mdadib@ukm.edu.my*

Received: 13 April 2017; Accepted: 17 April 2018

Abstract

Perovskites are materials that have many potential applications, such as humidity sensors, transparent conductive oxides, photocatalysts and capacitors. Strontium stannate ($SrSnO_3$) is a perovskite semi-conductor material with a wide band gap. Several synthesis methods are commonly used to form $SrSnO_3$, including solid-state reaction (SSR), sol-gel and hydrothermal. The SSR method requires high temperature calcination. On the other hand, sol-gel and hydrothermal methods merely need a lower calcination temperature to form perovskite materials. The sol-gel methods were done by adding a surfactant to $Sr(NO_3)_2$ and $SnCl_2$ solution in water before calcination. The autoclave approach was used in the hydrothermal method prior to calcination to form $SrSnO_3$. The objective of this study was to determine the morphological and optical properties of $SrSnO_3$ synthesized by sol-gel, hydrothermal and SSR. The band gap was calculated *via* Kubelka-Munk relations and were found to be 4.05 eV (hydrothermal), 5.50 eV (sol-gel) and 3.95 eV (SSR). Sol-gel methods showed the widest band gap for $SrSnO_3$. Optical results showed that there is a difference in terms of band gap for a perovskite synthesized by the different methods. Mass reduction analysis by TGA showed a sol-gel has mass loss of approximately 58% due to dehydration, which is more than for hydrothermally synthesized $SrSnO_3$. This reduction is higher than for $SrSnO_3$ synthesized by hydrothermal method. It was observed that different synthesis methods impact the optical properties and morphology of $SrSnO_3$ powders.

Keywords: perovskites, hydrothermal, sol-gel, band gap, solid-state reaction

Abstrak

Perovskit merupakan bahan yang mempunyai banyak potensi untuk digunakan sebagai penderia kelembapan, oksida konduktif lutsinar, fotomangkin dan kapasitor. Strontium stannat ($SrSnO_3$) adalah bahan separuh konduktif berstruktur perovskit dengan jurang jalur yang besar. Beberapa kaedah sintesis biasanya digunakan untuk membentuk $SrSnO_3$ termasuk tindak balas keadaan pepejal (SSR), sol-gel dan hidroterma. Kaedah SSR memerlukan penalaan suhu yang tinggi, manakala kaedah sol-gel dan hidroterma hanya memerlukan suhu pengkalsinan yang lebih rendah untuk membentuk bahan perovskit. Kaedah sol-gel dilakukan dengan menambah surfaktan pada larutan $Sr(NO_3)_2$ dan $SnCl_2$ dalam air sebelum pengkalsinan. Pendekatan autoklaf digunakan dalam kaedah hidroterma sebelum pengkalsinan untuk membentuk $SrSnO_3$. Objektif kajian ini adalah untuk menentukan morfologi dan ciri optik bagi bahan $SrSnO_3$ yang disintesis melalui kaedah sol-gel, hidroterma dan SSR. Jurang jalur telah dikira melalui hubungan Kubelka-Munk dan didapati nilainya adalah 4.05 eV (hidroterma), 5.50 eV (sol-gel) dan 3.95 eV (SSR). Kaedah sol-gel menunjukkan jurang jalur yang terbesar bagi $SrSnO_3$. Ciri optik menunjukkan wujudnya perbezaan antara jurang jalur bagi perovskit yang disintesis melalui kaedah yang berlainan. Analisa pengurangan jisim menggunakan TGA menunjukkan bahawa sol-gel mempunyai pengurangan jisim dianggarkan sebanyak 58% disebabkan penyahhidratan. Pengurangan ini adalah lebih tinggi berbanding dengan $SrSnO_3$ yang disintesis melalui kaedah hidroterma. Ia telah dilihat bahawa kaedah sintesis boleh memberi kesan pada ciri optik dan morfologi pada serbuk $SrSnO_3$.

Kata kunci: perovskit, hidroterma, sol-gel, julang jalur, tindak balas keadaan pepejal

Introduction

Strontium stannate ($SrSnO_3$) is a perovskite structured semi-conducting material with a wide band gap of 4.1 eV. It can also absorb light in the ultraviolet region [1, 2]. As such, it is a typical practice to introduce a dopant to the perovskite structure in order to allow the material to absorb a wider light spectrum and improve its conductivity. Besides having a wide band gap, perovskites possess many other interesting properties, such as superconductivity and colossal magnetoresistance. Perovskites like $MSnO_3$ (M = Sr, Ba, Ca) can be synthesized by several methods, and one of them is the solid-state reaction (SSR) method. This method involves mixing metal oxides in a mortar and then calcining at high temperatures. Liu et al. used this method to synthesize Sb doped $SrSnO_3$ by mixing tin oxide (SnO_2), strontium carbonate ($SrCO_3$) and antimony oxide (Sb_2O_3) into a mortar and calcining at ~1500 ˚C for 24 hours [3]. This method is relatively simple, but requires high calcination temperatures that consume a great deal of electricity [4].

Alternative methods with lower calcination temperatures include sol-gel and hydrothermal methods. The sol-gel method for synthesis of $SrSnO_3$ is a wet-chemical method that has been used to produce perovskite materials [5-7]. This method includes the use of metal nitrates, chlorides, acetates and other chemicals in a solution. The metal precursors are made into a solution and mixed with a surfactant to assist particle agglomeration and the perovskite formation reaction. The precursors and are surfactant stirred, heated and then dried before calcination. Kumar et al. synthesized Fe-doped $SrSnO_3$ by the sol-gel method and calcined at 650˚C for 2 hours [8]. This method requires a much lower calcination temperature for formation of $SrSnO_3$, but requires a more complicated synthesis [4].

Hydrothermal is another solution-oriented method. This method involves similar precursors used for sol-gel (metal salts, acetates, etc.), but also requires the use of an alkali and autoclave to form powders or nanorod perovskites [9, 10]. A study by Li et al. applied this method to synthesize $SrSnO_3$ nanorods by mixing SnCl, $Sr(NO_3)_2$ and cetyltrimethylammonium bromide (CTAB) in solution [11]. The solution was adjusted with NaOH drops until it reached a pH of 13. A suspension formed after reaching the said pH and it was transferred to an autoclave to be heated for several hours. The suspension was then calcined at 600 ˚C, or higher, for 3 hours until $SrSnO_3$ formed. This method was reported to have a low calcination temperature and result in fewer impurities in the product, but the use of autoclaves and long processing times make it less favourable for bulk production [12].

The purpose of the study is to synthesize $SrSnO_3$ using three different methods (SSR, sol-gel and hydrothermal) and characterize it in terms of morphology, optical properties and crystal quality. This study hopes to provide valuable insights into the three different methods of perovskite synthesis to aid in future studies of this material, as each method tends to give slightly different results to the final product.

Materials and Methods

No autoclave route (sol-gel)

The sol-gel method used for this study was based on Kumar et al. [8]. Reagent grade strontium nitrate with 99% purity ($Sr(NO_3)_2$), tin chloride with 98% purity ($SnCl_2$) and CTAB with >99% purity were obtained from Sigma Aldrich and added to 30 mL of deionized water. The solution was then stirred for 4 hours at 80˚C until the solution became a white gel. The gel was then dried at 100 ˚C on a hot plate in air until it transformed into a powder. The powder was washed with ethanol to reduce any remaining impurities and left to dry. The white powder, $SrSn(OH)_6$, was then calcined in the furnace at 650˚C for 2 hours until $SrSnO_3$ powder formed. The formation of $SrSnO_3$ can be described by the following equations 1 and 2:

$$Sr(NO_3)_2 + SnCl_2 + 4H_2O \rightarrow SrSn(OH)_6 + 2HCl + N_2 + 2O_2 \quad (1)$$

$$SrSn(OH)_6 \rightarrow SrSnO_3 + 3H_2O \quad (2)$$

Equation 1 describes the formation of $SrSn(OH)_6$ from the precursors and equation 2 shows the calcination of $SrSn(OH)_6$ to form the final product, $SrSnO_3$.

Autoclave route (hydrothermal)

A more detailed reaction route involving hydrothermal synthesis of $SrSnO_3$ can be found in Li et al. [11]. Strontium nitrate with 99% purity ($Sr(NO_3)_2$), tin chloride with 98% purity ($SnCl_2$) and CTAB with >99% purity were added to 30 mL deionized water and stirred. While stirring, NaOH 1 M was added, drop by drop, to the solution to maintain pH of 13 until a white suspension appeared. The suspension was placed in an autoclave and sealed for 16 hours at 160 ˚C. After the autoclave cooled to room temperature, the suspension turned into a white gel and was left to dry. When dried, the gel was a white coloured powder of $SrSn(OH)_6$. The powder was later calcined at 650 ˚C for 2 hours to form the $SrSnO_3$ powder.

Solid-state reaction route (SSR)

The SSR route used in this study was carried out based on James et al. [13]. Equimolar $SrCO_3$ and SnO_2 powders with 99% purity were obtained from Sigma Aldrich and mixed with a mortar and pestle. Acetone was added to the mixture to act as a binder for the powders. After mixing, the powder was transferred to a porcelain boat and calcined for 12 hours at 800˚C. The powder was then reground and calcined again at 850 ˚C for 18 hours. After the final grinding, the mixture was calcined once more at 900 ˚C for 24 hours. A white powder of $SrSnO_3$ was obtained after calcination. The simple solid-state reaction equation may be described by equation 3:

$$SrCO_3 + SnO_2 \rightarrow SrSnO_3 + CO_2 \quad (3)$$

Characterization

Thermogravimetric analysis (TGA) was done using a Perkin Elmer STA6000. The TGA-DSC testing was done under nitrogen with a heating rate of 10 ˚C/min at a temperature range of 30-1000 ˚C. X-ray diffraction (D8 Advance Bruker AXS Germany) with CuKα radiation was used to identify the crystal quality and crystal structure. UV-Vis spectroscopy data was obtained by diffuse reflectance at a wavelength range of 200-800 nm using a PerkinElmer UV/VIS/NIR Spectrometer Lambda 950. The morphology of the material was studied by using SEM Supra 55VP. X-ray Photoelectron Spectroscopy was done with Kratos/Axis Ultra delay-line detector (DLD).

Results and Discussion

Crystal structure

The XRD patterns for the $SrSn(OH)_6$ powders synthesized from the hydrothermal and sol-gel methods show the presence of hexagonal $SrSn(OH)_6$, as illustrated in Figure 1(a). These patterns were a match for a $SrSnOH_6$ precursor, according to database PDF00-009-0086. The peaks at 2θ values of 11˚, 20˚, 22˚, 28˚, 32˚, 36˚, and 41˚ corresponded to *hkl* numbers (Bragg reflection planes) of (110), (301), (004), (330), (512), (432) and (006), respectively. The lattice parameters, according to the PDF database, were $a = b = 16.35$ nm and $c = 12.34$ nm for the hydrothermal and sol-gel synthesized $SrSn(OH)_6$. The peaks were nearly identical to the peaks found in Li et al. [11], with minimal noise in the data. A similar peak for $SrSn(OH)_6$ was observed for both methods. However, there was an unknown peak at 5˚ for the sol-gel method. Meanwhile, there was an increased intensity for the (006) peak in hydrothermal route, which may correspond to deformity of the crystal structure.

The precursor powders from each route were calcined (with the exception of powders from SSR route) to produce the $SrSnO_3$ powders. The XRD spectra of the SSR, sol-gel and hydrothermal routes are shown in Figure 1(b). The XRD of powders via the hydrothermal route had a cubic crystal structure with lattice parameters of $a = b = c =$ 8.0682 according to PDF00-022-1442. The peaks are at 2θ values of 22˚, 25.2˚, 31.5˚, 44.5˚, 50.5˚, 55.5˚, 65.3˚, 70˚ and 74.3˚ and correspond to reflection planes of (200), (210), (220), (400), (420), (422), (440), (600) and (620), respectively. When compared to the patterns of the hydrothermally synthesized $SrSn(OH)_6$ precursors, it can be seen that the patterns have slight differences, due to the formation of the $SrSnO_3$ product from its precursors. The sol-gel synthesized $SrSnO_3$ powder also possesses similar notable peaks, but the presence of unknown peaks increased, and may indicate that more impurities were present that affected the crystal structure. The SSR synthesized $SrSnO_3$ has fewer unknown peaks at lower 2θ compared to the sol-gel method. Based on these spectra, all methods can produce $SrSnO_3$ with the correct perovskite crystal structure. The crystal quality, in terms of impurity presence in the $SrSnO_3$, was best for the hydrothermal method, followed by SSR. The sol-gel method was observed to have the highest impurities due to having multiple unknown diffraction peaks.

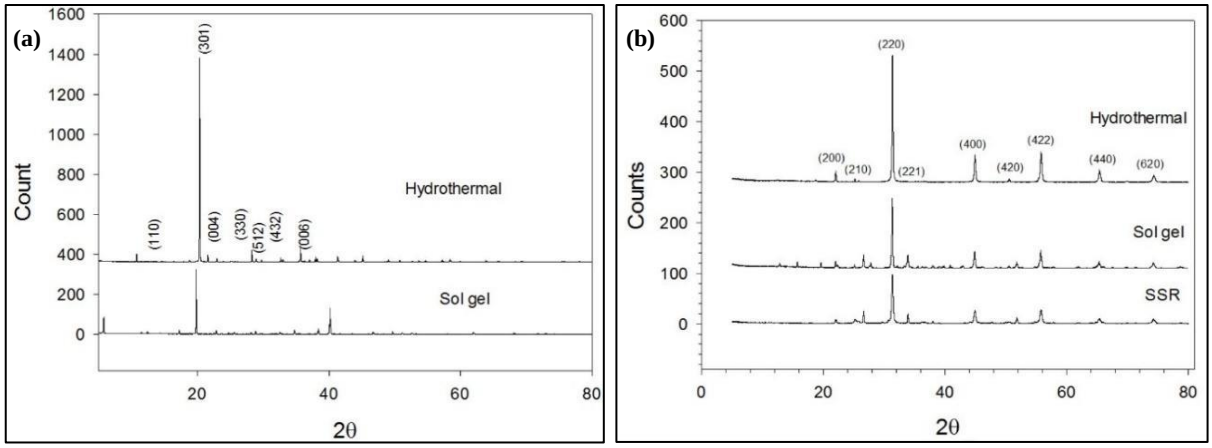

Figure 1. XRD spectra of (a) $SrSn(OH)_6$ and (b) $SrSnO_3$

Thermogravimetric analysis (TGA)

TGA analysis of $SrSn(OH)_6$ was done on the hydrothermal and sol-gel routes only. This analysis was done to determine whether the solutions formed correctly, if dehydration occurred and at what temperatures. This was not possible for the SSR route because the precursor oxides crystallized directly to $SrSnO_3$ instead of forming $SrSn(OH)_6$. The TGA for hydrothermal and sol-gel synthesized $SrSnO_3$ was done for the temperature range of 50 – 1000 ˚C, as shown in Figure 2.

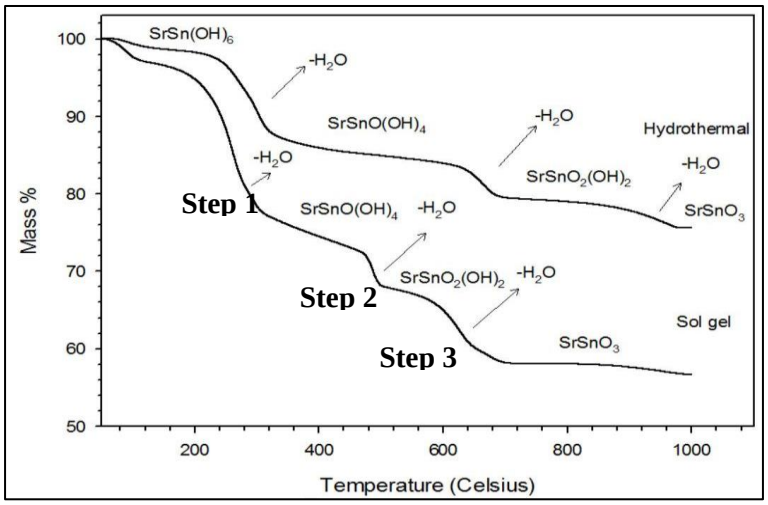

Figure 2. TGA analysis of $SrSn(OH)_6$ reduction into $SrSnO_3$

The $SrSn(OH)_6$ synthesized by the hydrothermal route also experienced mass reduction due to water evaporation. The minimum mass percent obtained after the analysis was ~78% of the original mass. The first 13% weight loss occurred at the temperature range of 230 – 350 ˚C. The second 3% mass reduction occurred at the temperature range of 630 – 690˚C of. The last ~2% weight loss due to evaporation occurred at 920 – 970˚C. The $SrSn(OH)_6$ powders synthesized by the sol-gel method experienced step-by-step weight loss to a minimum remaining mass percent of ~56%. A very small 3% weight loss occurred at ~88˚C and minor reductions occurred up to 190˚C. The 3% weight loss suggests that the water (H_2O) content was beginning to be removed from the material. There was a sudden mass drop of 17% at temperatures between 205 – 320˚C, which is where a large amount H_2O evaporated. The second notable H_2O evaporation occurred at 480 –500˚C and resulted in a weight loss of 5%. The last mass reduction of 6%

occurred at 610 ˚C and no more mass reduction occurred for temperatures greater than 700˚C. This suggests that at this temperature, $SrSn(OH)_6$ was dehydrated and 48% of its mass was reduced to finally form $SrSnO_3$. These three stages of weight loss due to hydration are in agreement with published literature [8]. Thus, the sol-gel method synthesized $SrSnO_3$ yielded less after exposure to high temperatures compared to hydrothermally synthesized $SrSnO_3$. The three steps of $SrSn(OH)_6$ dehydration maybe be represented by equations:

Step 1 - $SrSn(OH)_6 \rightarrow SrSnO(OH)_4 + H_2O$ (4)
Step 2 - $SrSnO(OH)_4 \rightarrow SrSnO_2(OH)_2 + H_2O$ (5)
Step 3 - $SrSnO_2(OH)_2 \rightarrow SrSnO_3 + H_2O$ (6)

Diffuse reflectance and band gap estimation

UV-Vis measurements were done on the $SrSnO_3$ powders synthesized by the different routes. The diffuse reflectance was obtained, as shown on Figure 3(a), and then converted into the Kubelka-Munk function for band gap determination [14]. Based on Figure 3(b), the band gap of hydrothermal, sol-gel and SSR synthesized $SrSnO_3$ was found to be 4.05 eV, 5.5 eV and 3.95 eV, respectively. The band gap of $SrSnO_3$ has been reported to be 4.1 eV in the literature [1, 8]. It can be seen that the band gap for hydrothermally prepared $SrSnO_3$ is closest to the value in the literature, followed by sol-gel and SSR. Sol-gel has the highest band gap and its value differs from the literature. This could mean that the $SrSnO_3$ powders made by sol-gel have more impurities (supported by XRD pattern), thus resulting in higher band gap.

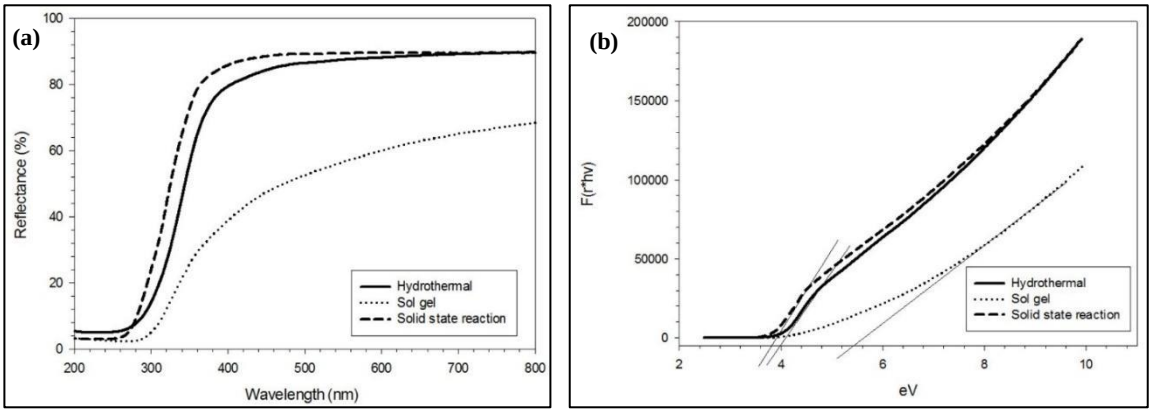

Figure 3. The optical analysis of $SrSnO_3$ (a) Reflectance spectra and (b) Diffuse reflectance transferred to Lubelka-Munk function for band gap determination [14]

Surface morphology

Figure 4(a) shows the SEM image for hydrothermally synthesized $SrSnO_3$. The $SrSnO_3$ was in the form of long cylinders, and a similar structure was also obtained by Li et al. [11]. This $SrSnO_3$ structure formation was due to NaOH reacting with $SnCl_4$ to form a $Sn(OH)_4$, which is able to dissolve in large amounts of NaOH and form $Sn(OH)_6^{2-}$ groups. This group reacts with cetyltrimethylammonium ion (CTA^+) from CTAB, forming CTA^+-$Sn(OH)_6^{2-}$ groups that allow crystals of $Sn(OH)_6^{2-}$ to grow along the orientation of the CTA^+ head group. Since the crystal has a direction to grow along the CTA^+ head group, this resulted in the crystals growing as rods, possibly long after the nucleation process in the autoclave [11]. Figure 4(b) shows the image of $SrSnO_3$ made by the SSR method. The powders have irregular sizes but are roughly similar in terms of shape. Sol-gel synthesized $SrSnO_3$, as shown in Figure 4(c), has larger powder clumps with a slightly irregular shape. The large powder clumps are due to the CTAB, which allows the growth of the crystals in all directions [13]. Based on these images, it would seem $SrSnO_3$ made by hydrothermal synthesis possesses a more uniform shape compared to the other methods that formed long shapes with varying sizes.

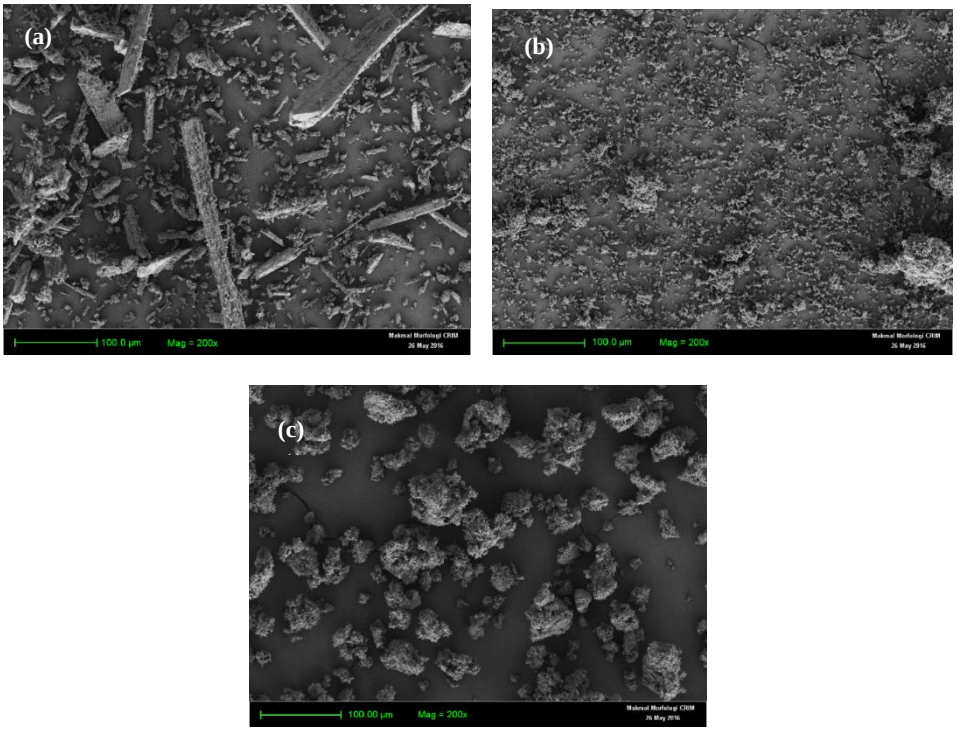

Figure 4. FESEM images at magnification of 200x of (a) hydrothermally synthesized $SrSnO_3$, (b) SSR synthesized $SrSnO_3$ and (c) sol-gel synthesized $SrSnO_3$

XPS spectra

Figure 5(a) shows the XPS spectra of O 1s in $SrSnO_3$ synthesized by the three methods. The hydrothermal method only has one peak present at 528 eV, where the O 1s is part of the main lattice of $SrSnO_3$ and the shoulder at 526.7 eV indicates the hydrated oxide species present in the sample, according to Kumar et al. [8]. The O 1s in the sol-gel has a vaguely visible peak at 528.7 eV. This small peak may indicate that only a small amount of O 1s was incorporated into the main lattice. The very small shoulder at 527.8 eV is the hydrated oxide species. The SSR $SrSnO_3$ has only one high peak for O 1s at 528.8 eV, and this indicates O 1s was well incorporated into the main $SrSnO_3$ lattice. Since the SSR method did not involve additional solutions or hydrates, there are no shoulders or peaks indicating that hydrated oxide species were present [8].

Figure 5(b) shows the Sn 3d peak for $SrSnO_3$. Two visible peaks are present for all $SrSnO_3$ synthesis methods. The first peaks at 483 – 484 eV for all methods indicate Sn $3d_{5/2}$. The second peak at ~492 eV for all methods corresponds to Sn $3d_{3/2}$. Both peaks are in accordance with the literature as Sn $3d_{5/2}$ and Sr $3d_{3/2}$ [15]. The peaks are highest for SSR followed by hydrothermal and sol-gel. The lowest peaks for the sol-gel method indicate that the Sn $3d_{5/2}$ and Sr $3d_{3/2}$ incorporation in the main lattice is less visible. Figure 5(c) shows the Sr $3d_{5/2}$ and Sr $3d_{3/2}$ peaks for $SrSnO_3$ produced by the three methods. Hydrothermal synthesized $SrSnO_3$ has peaks at 130.6 eV and 132 eV for Sr $3d_{5/2}$ and Sr $3d_{3/2}$, respectively. Sol-gel synthesized $SrSnO_3$ has Sr $3d_{5/2}$ and Sr $3d_{3/2}$ peaks at 132 and 133.5 eV, respectively. Finally, SSR has the highest peaks for Sr $3d_{5/2}$ and Sr $3d_{3/2}$ at 130.8 and 132.5 eV, respectively. According to these results, all have 2 peaks within 130 – 134 eV binding energy values, which corresponds to Sr^{2+} [15]. However, the variance in each spectrum of the three methods may suggest that the quality of Sr^{2+} bonding with main lattice is different, with SSR having the highest peak followed by sol-gel and hydrothermal. Overall, from the XPS spectra, SSR showed the most incorporation of each species (O 1s, Sr 3d and Sn 3d) into the main $SrSnO_3$ lattice, followed by hydrothermal and sol-gel.

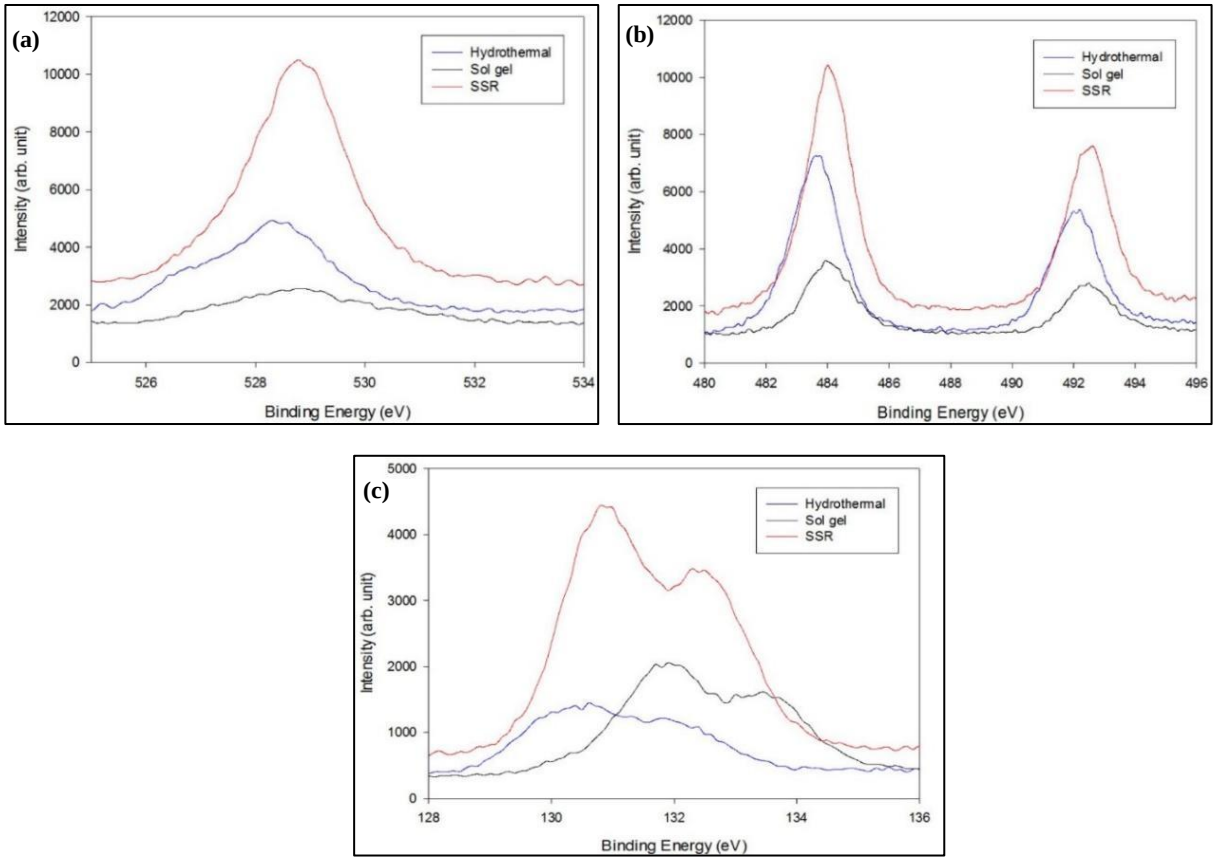

Figure 5. XPS spectra of $SrSnO_3$ synthesized via hydrothermal, sol-gel and SSR for (a) O 1s, (b) Sn 3d and (c) Sr 3d

Synthesis yield

Each synthesis method should produce different amounts of $SrSnO_3$ due to the different precursors used. All precursor solutions used had a basis of 10 mmol. Table 1 shows the yield percent of $SrSnO_3$ obtained after synthesis by the three different methods. Yield percentage is calculated by equation 7:

$$\text{Yield percent (\%)} = \frac{\text{Actual mass (g)}}{\text{Theoretical mass (g)}} \quad (7)$$

Table 1. Yield performance of $SrSnO_3$ obtained from three different synthesis methods

Synthesis Method	**$SrSnO_3$ Actual Yield Obtained (g)**	**Theoretical Yield**	**Yield%**
Hydrothermal	0.860	2.543	33.8%
Sol-gel	1.383	2.543	54.4%
Solid State Reaction (SSR)	2.176	2.543	85.6%

The SSR method yielded better by producing more $SrSnO_3$ powder, and this is why this method is still preferable in other studies [13, 16, 17]. Since this method uses powders only and not solvents, the yield is maximized. This

means that the weight of the total precursor oxides is close to the weight of the final product. Sol-gel produced the second highest yield. It produced more than the hydrothermal method because no filter or decanting was required since the solution was only heated and dried in same beaker. It was then only transferred once to the crucible for calcination.

Hydrothermally synthesized $SrSnO_3$ produced the least compared to SSR and sol-gel. The low yield was mainly due to the precursor solution being mixed with NaOH that mostly filled space in the autoclave container. Another factor would be loss of some main product $SrSn(OH)_6$ while filtering the solution from the autoclave. The difficulty of obtaining the product suspensions in the autoclave by scraping with a spatula also contributed to the loss of mass. Due to this difficulty, even though TGA analysis revealed that hydrothermal should yield more than sol-gel, the actual obtained yield was less.

Conclusion

The $SrSnO_3$ has been successfully synthesized *via* hydrothermal, sol-gel and SSR methods. The SEM showed that hydrothermal synthesized $SrSnO_3$ had the most regular and uniform particle shapes in the form of nanorods, followed by SSR and sol-gel. The TGA analysis showed both hydrothermal and sol-gel synthesized $SrSnO_3$ followed a 3-step dehydration process, with final minimum masses of 78% and 48% for hydrothermal and sol-gel, respectively. The hydrothermal and SSR methods had measured band gaps of 4.05 eV and 3.95 eV, respectively, which is close to the band gap value of 4.1 eV found in the literature. X-ray diffraction patterns and X-ray photoelectron spectra revealed the formation of orthorhombic phase $SrSnO_3$ nanoparticles through the three different synthesis methods. The XRD showed that $SrSnO_3$ with the least impurities was the hydrothermally synthesized $SrSnO_3$, followed by SSR and sol-gel. The XPS spectra of the $SrSnO_3$ produced by the SSR method showed a high binding energy intensity that indicated that each element was well incorporated into main lattice. The SSR method was followed by hydrothermal and sol-gel. In conclusion, $SrSnO_3$ can be produced using a low-cost method that results in some advantageous and disadvantageous material properties. With this option, the various dopants can be applied to the $SrSnO_3$ material to enhance some of its properties.

Acknowledgement

This work was supported by the Ministry of Higher Education, Malaysia and the research grant from Universiti Kebangsaan Malaysia (UKM) (Grant: GUP-2015-023).

References

1. Chen, H. and Umezawa, N. (2014). Sensitization of perovskite strontium stannate $SrSnO_3$ towards visible-light absorption by doping. *International Journal of Photoenergy*, 2014: 3–6.
2. Dohnalová, Ž., Gorodylova, N., Šulcová, P. and Vlček, M. (2014). Synthesis and characterization of terbium-doped $SrSnO_3$ pigments. *Ceramics International*, 40: 12637–12645.
3. Liu, Q., Dai, J., Zhang, X., Zhu, G., Liu, Z. and Ding, G. (2011). Perovskite-type transparent and conductive oxide films: Sb- and Nd-doped $SrSnO_3$. *Thin Solid Films*, 519(18): 6059–6063.
4. Ecija, A., Vidal, K., Larrañaga, A., Ortega-san-martín, L., Arriortua, M. I., Euskal, V. and Ehu, U. (2012). Synthetic methods for perovskite materials – structure and morphology. *Advances in Crystallization Processes*, 19: 485–505.
5. Para, T., Reshi, H. A. and Shelke, V. (2016). Synthesis of $ZnSnO_3$ nanostructure by sol gel method. *AIP Conference Proceedings*, 1731: 1–4.
6. Shan, C., Huang, T., Zhang, J., Han, M., Li, Y., Hu, Z., & Chu, J. (2014). Optical and electrical properties of sol − gel derived Ba−$LaSnO_3$ transparent conducting films for potential optoelectronic applications. *The Journal of Physical Chemistry C*, 118(13): 6994-7001.
7. Xu, K., Yao, M., Chen, J., Zou, P., Peng, Y., Li, F. and Yao, X. (2015). Effect of crystallization on the band structure and photoelectric property of $SrTiO_3$ sol–gel derived thin film. *Journal of Alloys and Compounds*, 653: 7–13.
8. Kumar, A., Quamara, J., Dillip, G., Joo, S. and Kumar, J. (2015). Fe(III) induced structural, optical, and dielectric behavior of cetyltrimethyl ammonium bromide stabilized strontium stannate nanoparticles synthesized by a facile wet chemistry route. *RSC Advance*, 5(22): 17202–17209.

9. Chen, C., Cheng, J., Yu, S., Che, L. and Meng, Z. (2006). Hydrothermal synthesis of perovskite bismuth ferrite crystallites. *Journal of Crystal Growth*, 291(1): 135–139.
10. Li-Jie, H., Dong, Z., Shou-hua, F., Bo, Z. and Gang, C. (2012). Hydrothermal synthesis and characterization of perovskite oxide $AgTaO_3$. *Chemical Research in Chinese Universities*, 28: 760–763.
11. Li, C., Zhu, Y., Fang, S., Wang, H., Gui, Y., Bi, L. and Chen, R. (2011). Preparation and characterization of $SrSnO_3$ nanorods. *Journal of Physics and Chemistry of Solids*, 72(7): 869–874.
12. Ahmadi, S., Asim, N., Alghoul, M., Hammadi, F., Saeedfar, K., Ludin, N. and Sopian, K. (2014). The role of physical techniques on the preparation of photoanodes for dye sensitized solar cells. *International Journal of Photoenergy*, 2014: 1-19.
13. James, K., Aravind, A. and Jayaraj, M. (2013). Structural, optical and magnetic properties of Fe-doped barium stannate thin films grown by PLD. *Applied Surface Science*, 282: 121–125.
14. Bellal, B., Hadjarab, B., Bouguelia, A. and Trari, M. (2009). Visible light photocatalytic reduction of water using $SrSnO_3$ sensitized by $CuFeO_2$. *Theoretical and Experimental Chemistry*, 45(3): 160–166.
15. Junploy, P., Thongtem, T., Thongtem, S. and Phuruangrat, A. (2014). Decolorization of methylene Blue by $Ag/SrSnO_3$ composites under ultraviolet radiation. *Journal of Nanomaterials*, 2014: 67.
16. Kotan, Z., Ayvacikli, M., Karabulut, Y., Garcia-Guinea, J., Tormo, L., Canimoglu, A. and Can, N. (2013). Solid state synthesis, characterization and optical properties of Tb doped $SrSnO_3$ phosphor. *Journal of Alloys and Compounds*, 581: 101–108.
17. Liu, Q., Wang, H., Chen, F. and Wu, W. (2008). Single-crystalline transparent and conductive oxide films with the perovskite structure: Sb-doped $SrSnO_3$. *Journal of Applied Physics*, 103(9): 93709.